Marine Biotechnology (2022) 24:18–31
https://doi.org/10.1007/s10126-021-10083-y

ORIGINAL ARTICLE

Genome-Wide Differential DNA Methylomes Provide Insights into the Infertility of Triploid Oysters

Dongfang Sun[1] · Hong Yu[1,2] · Qi Li[1,2]

Received: 23 July 2021 / Accepted: 3 November 2021 / Published online: 18 January 2022

Abstract

Chromosomal incompatibility and gene expression changes would affect the development of polyploid gonad and gamete formation. The role of epigenetics like DNA methylation in reproductive development is fully demonstrated in diploid animals. The lack of polyploid species and the infertility of polyploid animals, especially the odd ploidy, limit the study of epigenetic regulation mechanism of polyploid reproduction. Fertile and infertile individuals exist in triploid Pacific oyster *Crassostrea gigas*, which provide an interesting model for studies on the effect of epigenetic regulation on gonadal development. The whole genome single base resolution DNA methylomes in gonads of triploid females α (F-3nα), triploid females β (F-3nβ), triploid males α (M-3nα), triploid hermaphrodite predominantly males (HPM-3n), diploid females (F-2n), and diploid males (M-2n) were generated by using bisulfite-sequencing. The overall DNA methylation profiles in gene regions and transposable regions of fertile and infertile triploid oysters were consistent with those of diploid oysters. The DNA methylation level of CG context decreased in infertile triploid oysters, with more hypomethylated than hypermethylated regions, and the opposite is true in fertile triploid oysters. Genes harbored with differentially methylated regions (DMRs) in infertile triploids were mainly related to the metabolism pathways and the signal pathways. Correlation analysis indicated that the expression of gene transcriptions was generally positively associated with DNA methylation in gene body regions, and DMRs in infertile triploid oysters played significant roles in gonadal development as a possible critical epigenetic regulator of gonadal development gene transcriptional activity. These findings indicate a potential relationship between DNA methylation variability and gene expression plasticity in newly formed polyploidy. As far as we know, this is the first study revealing the epigenetic regulation of gonadal development in invertebrates based on fertile and infertile models, meanwhile providing a new mentality to explore the regulatory mechanisms of infertility in triploids.

Keywords DNA methylation · Gonadal development · Infertility · Triploid oysters

Introduction

Polyploidy have always been regarded as an important evolutionary phenomenon. It is common in plants while rare in animals, which may be related to the incompatibility of complex developmental and reproductive patterns (Mable 2004; Wertheim et al. 2013). However, the occurrence frequency of polyploidy in certain groups such as fish and amphibian is relatively high (Otto and Whitton 2000; Pala et al. 2008). Polyploidy events cause great changes in genome structure and cell tissues, which raised important challenges to cell cycle process (such as meiosis and mitosis), cell physiology (such as growth and metabolism), and the regulation of gene transcription and genomic stability (Wertheim et al. 2013). Epigenetic modifications like DNA methylation can be triggered by environmental stimuli or genomic pressure like polyploidization, affecting overall gene expression patterns and altering plasticity of the new polyploid genome (Wertheim et al. 2013; Siegfried and Simon 2010). For instance, in plants, the formation of triploids is accompanied by a large number of genetic and DNA methylation variations, which illustrate the heterosis

Dongfang Sun and Hong Yu contributed equally to this work.

✉ Qi Li
qili66@ouc.edu.cn

[1] Key Laboratory of Mariculture, Ministry of Education, Ocean University of China), Qingdao 266003, China

[2] Laboratory for Marine Fisheries Science and Food Production Processes, Qingdao National Laboratory for Marine Science and Technology, Qingdao 266237, China

phenotype of triploid loquat (Liu et al. 2018); switchgrass autopolyploidization changes phenotype and flowering time through epigenetics and regulation of gene expression (Yan et al. 2019). In mammals, DNA methylation inhibits gene expression on one X chromosome, indicating that different epigenetic states can achieve transcriptional compensation related to ploidy variation (Conrad and Akhtar 2012; Schultz et al. 2015); in ants, phenotypic changes caused by differences in the female and male genomes are associated with DNA methylation, which is related to selective splicing and gene expression (Bonasio et al. 2012).

The Pacific oyster (*Crassostrea gigas*) is one of the most important marine invertebrates for the economic value and biological characteristics. Crossing between tetraploid and diploid oysters can produce triploid oysters, and triploidy also can be induced through chemical mechanisms (Guo et al. 1996). Compared with diploid oysters, most triploid oysters have blocked gonadal development and are sterile. However, a few triploids can generate aneuploid gametes and develop into viable offspring (Guo and Allen 1994). The triploid oysters that can produce a large number of gametes are called 3nα, and the triploid oysters that can generate few gametes are called 3nβ (Jouaux et al. 2010). The three sets of chromosomes in triploid oyster cause important pressure factors for the maintenance of the structure and function of organism genome and the effect of dose compensation (Birchler et al. 2007; Hegarty et al. 2011; Madlung 2013). The phenomenon of fertility and infertility exists in triploid oysters, which means that triploid oysters are the perfectly suited model for us to study the effect of ploidy on gonadal development. At present, two main opinions about the mechanism of sterile triploids: at the chromosomal level, defect of chromosome pairing in meiosis leads to gamete failure (Piferrer et al. 2009; Spangenberg et al. 2017); at the transcription level, fertile triploid oysters show that gonadal growth retardation is related to cell cycle checkpoint (Dheilly et al. 2014). In comparison with the diploid parent, triploid oysters simply have an extra set of chromosomes and not many changes in DNA sequence. Transcriptome analysis revealed that the regulatory network between triploids and diploids was altered, inducing generous alterations in gene expression (Dheilly et al. 2014). This means that an increase in chromosome number leads to changes in gene expression that affect phenotypic changes. However, information about what controls these changes in gene expression is still scarce.

The normal development of gonads is the most fundamental condition for the continuation of gamogenetic species. The maturation of the gonads of *C. gigas* is accompanied by a large number of gene expression variation (Dheilly et al. 2014; Cavelier et al. 2017; Yue et al. 2018), and the genome is marked difference in the pattern of methylation across gametogenesis between female gonads and male gonads (Zhang et al. 2018). Methylation and demethylation are also accompanied with the whole process of fruit from development to maturity in the stages of gonadal development in plants (Lang et al. 2017; Zhong et al. 2013). In these processes, several keys, evolutionarily conserved enzymes known collectively as DNA methyltransferases and demethylases, are required to write and erase DNA methylation, so the difference of methylation may be the result of the interaction of DNA methyltransferases and demethylases (Okano et al. 1999; Ribas et al. 2017). In polyploidy, genome replication increases the complexity of chromosome structure and gene interaction networks. It is necessary to re-establish genome balance both at a chromosome structure level and at a gene expression level to ensure the normal procedures of gonadal development (Wertheim et al. 2013; Soltis and Soltis 1999). The effect of epigenetic variation on gonadal development also is an interesting enough question in polyploidy, with the exception of chromosome pairing defect and gene expression difference that led to polyploid reproductive disorder (Dheilly et al. 2014).

In this study, we obtained genome-wide methylomes and transcriptomes data of fertility and infertility oysters using whole-genome bisulfite sequencing (WGBS) and RNA sequencing (RNA-seq). To reveal the mechanism of epigenetic modification in sterility triploids, the DNA methylomes of fertility diploid and infertility triploid oysters were compared. We also performed a correlation analysis of gene transcription and DNA methylation to reveal the relationship between DNA methylation and gene expression.

Materials and Methods

Animals

In this study, triploid oysters were generated by mating diploid females and tetraploid males in a private hatchery in 2017. We tried to find the male 3nβ sterile individuals. Unfortunately, we observed the gonads of more than 1500 triploid oysters by hematoxylin–eosin staining method and failed to find the male 3nβ, but a few male-dominated hermaphrodites were found. The male-dominated hermaphrodites were sterile and the phenotypic characteristics were similar to male 3nβ. All the experimental animals were dissected after anesthesia. Ploidy of diploid female oysters (F-2n), diploid male oysters (M-2n), α and β pattern of triploid female oysters (F-3nα and F-3nβ), α pattern of triploid male oysters (M-3nα), and triploid hermaphrodite predominantly males (HPM-3n) were detected by flow cytometry, and gonadal staging and gender determination were performed by histology (Jouaux et al. 2010). For each of the six samples (F-2n, M-2n, F-3nα, F-3nβ, M-3nα, and HPM-3n), three biological replicates were utilized at the maturing stages. The gonads were also collected

at different stages (resting, proliferating, and maturing stages), and three biological replicates were utilized to detect the dynamic expression of epigenetic factors.

Whole-Genome Bisulfite Sequencing and Data Analysis

The whole-genome bisulfite sequencing libraries were prepared by using the gonads of 18 oysters. Briefly, genomic DNAs isolated from the gonads were segmented into 100–300 bp by sonication (Covaris, USA) and purified with PCR Purification Kit (QIAGEN, USA). The DNA fragments were terminal repaired, and the "A" nucleotide was added to the 3′ terminal of the blunt fragments. The DNA fragments were then ligated to methylated sequencing adapters. Fragments with adapters were bisulfite treated with MethylationGold kit (ZYMO, USA). Finally, the DNA fragments treated with sodium bisulfite were amplified by PCR and sequenced using Illumina HiSeqTM 2500 by Gene Denovo Biotechnology Co. (Guangzhou, China). Lambda DNA was mixed in each sample as a conversion quality control for each library.

The Lambda genome was merged with the reference genome of *C. gigas* so that reads originating from the unmethylated control DNA could be aligned. Reads treated with bisulfite were mapped to the reference genome using BSMAP (version: 2.90) software by default (Xi and Li 2009). mCs were determined according to the modified algorithm of Lister et al. (2009). The DNA samples used for analysis were multi-cell samples, so the methylation level of C base was in the range of 0 ~ 100%, which is equal to the sum of the methylation levels of effective covering C base divided by the total number of effective covering bases. The formula for calculating the methylation level of a single site was as follows:

$$\text{Methylation level of single locus} = 100 * \frac{\text{(number of sequences covered to mC)}}{\text{(total number of effective sequences covered)}}.$$

The methylation level was calculated based on the percentage methylated cytosine in the total genome, in various regions of the genome for CG, CHG, and CHH context. In order to evaluate different methylation profiles in different genomic regions, the methylation profile of upstream 2-kb regions (from 2 kb upstream to the transcription start site), downstream 2-kb regions (from the transcription end site to 2 kb downstream), and gene body (from transcription start site to transcription end site) was plotted according to the average methylation level of each window. The minimum read coverage to call a methylation status for a base was set to 4 to identify DMRs between two samples. DMRs were performed for each sequence context (CG, CHG, and CHH) according to different criteria: (1) For CG, more than five GC sites in each window, absolute value of the methylation rate difference was more than 0.25, and $q \leq 0.05$. (2) For CHG, more than five CHG sites in a window, absolute value of the methylation rate difference was more than 0.25, and $q \leq 0.05$; 3). For CHH, more than fifteen CHH sites in a window, absolute value of the methylation rate difference was more than 0.15, and $q \leq 0.05$.

Functional Enrichment Analysis of DMR-Related Genes

KEGG (http://www.kegg.jp/kegg/) analysis was carried out to examine which biological and physiological pathways might be influenced by DMRs. KEGG pathway enrichment analysis was performed for the genes with DMRs by means of KOBAS software (Mao et al. 2005), and corrected $P < 0.05$ were considered significantly enriched by DMR-related genes.

RNA-seq and Data Analysis

Total RNAs were extracted from 100 mg of 18 gonads used above using TRIzol reagent (Invitrogen). We removed the rRNAs from the samples and retained only mRNAs and non-coding RNAs. The RNA-seq libraries were built based on Illumina's standard protocol, and the libraries were sequenced on an Illumina HiSeq™ 2500 RNA-sequencer at Gene Denovo Biotechnology Co. (Guangzhou, China). Bowtie2 was used to map the reads against the ribosome RNA (rRNA) database to delete rRNA mapped reads. TopHat 2 v2.0.3.12 package with default settings was employed to map the transcriptome reads to the reference genome. RSEM v1.2.19 package was used to quantify the abundance of each transcript, and FPKM (Fragments per kb per Million reads) was used to normalize the transcript expression levels.

Correlation of DNA Methylation and Gene Transcription

To detect whether gene expression influences DNA methylation in a sample, genes were categorized into four classes based on their transcription levels, including a non-expressed group (FPKM ≤ 1), a low-expressed group (1 < FPKM ≤ 10), a middle-expressed group (10 < FPKM ≤ 100), and a high-expressed group (FPKM > 100).

To analyze whether DNA methylation influences gene transcription in a sample, genes were categorized into four classes

Table 1 Average statistic of WGBS for each sample

Samples	Total reads	Mapped reads	Mapped ratio (%)	Sequence depth	Bisulfite conversion rate (%)
F-3nα	359,157,576	206,634,371	57.53	55.28	99.19
F-3nβ	354,027,330	206,291,768	58.24	55.21	99.28
M-3nα	348,345,946	201,446,871	57.84	53.91	99.31
HPM-3n	326,353,376	187,066,133	57.30	50.06	99.25
F-2n	333,235,848	188,269,320	56.57	50.38	99.25
M-2n	341,028,394	199,780,996	58.57	53.46	99.42

*Each sample contains three replicates

according to their methylation level, including a non-methylation group, a low-methylation group, a middle-methylation group, and a high-methylation group (gene-excluded non-methylation was divided into 3 groups on average). The relationship between DNA methylation and gene transcription in ± 2 kb flanking regions and gene body region was statically analyzed by Spearman's correlation analysis. rho > 0 ($P < 0.05$), means positive association; rho < 0 ($P < 0.05$), means negative association.

Gene Expression and Transcriptome Validation by qRT-PCR

To detect the expression pattern of methylation related genes in different gonadal development stages and validate the differentially expressed genes (DEGs), total RNAs of three individuals for each sample in each development stage were isolated using TRIzol reagent (Invitrogen) according to previous description. The first strand of cDNA was synthesized using PrimeScript™ RT reagent Kit (Takara) according to the direction of manufacturer. Primers used in this study were designed using the Primer 5 software (Table S1). *Ef1α* was chosen for the internal reference gene. EvaGreen 2 × qPCR Kit (abm) was used for qPCR test according to the manufacturer's protocol and using LightCycler 480 (Roche) RT-PCR instrument. The relative expression was calculated by using the $2^{-\Delta\Delta CT}$ method. Analysis of variance (ANOVA) for significance test and $P < 0.05$ indicated a significant difference.

DNA Methylation Validation by BSP

The bisulfite conversion kit (NEB) was used to process the sample genome according to the instructions. The target fragment was amplified using LA taq enzyme (TaKaRa), then the target fragment was ligated to the vector pMD19-t (TaKaRa). Randomly pick ten clones for each sample for sequencing. Software BiQ_Analyzer was used to analyze the sequencing results and graph.

Statistical Analysis

Methylation level data were presented as mean ± standard error, and significance test was performed by ANOVA. The Spearman correlation and significance test were carried out by using cor.test in R software.

Results

DNA Methylation Patterns of Gonads in Oysters

In order to evaluate the DNA methylation patterns of different ploidies and the epigenetic mechanism of triploids sterility, we carried out WGBS on bisulfite-converted DNA isolated from gonads of triploid females α (F-3nα), triploid females β (F-3nβ), triploid males α (M-3nα), and triploid hermaphrodite predominantly males (HPM-3n). The gonads of diploid females (F-2n) and diploid males (M-2n) were sequenced as the control groups. Moreover, the corresponding samples were sequenced to determine gene expression. All the rawdata of WGBS and RNA-seq were available at the NCBI under the project number PRJNA684407 and PRJNA690125, respectively.

In total, each sample generated an average of 344 million reads, which yielded an average depth of 53 × per strand, and an average of 198 (58%) millions reads from each sample (Table 1) could be aligned to the oyster genome (unpublished). The bisulfite conversion rate (%) of all sequencing libraries ranges from 99.19 to 99.42% (Table 1). Approximately 75% of genomic cytosines (Cs) were covered by at least one read (Tables 2 and S2). An average of 6.4 million methylated cytosines (mCs) were discovered in the genomic DNA extracted from gonads in each sample, which accounted for 2.20% of Cs in the reference genome (Table 3). Ultimately, we observed genome-wide methylation levels of 14.27% at CG sites, 0.52% at CHG sites, and 0.51% at CHH sites. More than 87% of mCs were in mCG context, and mCHG and mCHH accounted for 2.58% and 9.57% of mCs, respectively (Table 3).

DNA Methylation Profiles in Gene and Transposable Element (TE) Regions

In order to detect the DNA methylation profiles of genes encoding protein, we analyzed three conventional

Table 2 Average ratio of cytosines covered by at least one unique read in each context

Sample*	Covered cytosines (%)			
	C	CG	CHG	CHH
F-3nα	76.48	76.43	78.51	76.11
F-3nβ	76.85	76.79	78.53	76.48
M-3nα	76.98	76.79	78.52	76.66
HPM-3n	75.55	75.51	77.22	75.18
F-2n	71.42	71.01	72.94	71.14
M-2n	73.81	73.46	75.44	73.51

*Each sample contains three replicates

methylation contexts: gene body regions, the upstream-2 k regions and downstream-2 k regions (Wang et al. 2014, 2021) in all the samples. Interestingly, the overall DNA methylation profiles were consistent in both diploid and triploid oysters in gene body regions (Figs. 1A and S1A–E). The upstream 5′ region of the gene near the initiation of the coding sequence presented low levels of methylation at CG sites. Subsequently, the methylation levels increased and showed high methylation levels in the gene body regions, and then the methylation level gradually decreased near the downstream 3′ region (Fig. 1A). Moreover, the methylation level of 3′UTR was higher than that of 5′ UTR, and exon methylation level was higher than that of intron (Fig. 1A, B). However, the methylation patterns of CHG and CHH sites with low methylation levels did not fluctuate in the gene regions (Fig. S1F).

Table 3 Methylated cytosines detected in each sample

Sample*	Context	Number of modified sites	Methylation level (%)	Methylation proportion of the aligned genome (%)
F-3nα	C	6,756,154	2.25	100
	CG	5,890,884	13.83	87.20
	CHG	182,700	0.62	2.70
	CHH	682,570	0.63	10.1
F-3nβ	C	6,448,917	2.07	100
	CG	5,742,094	13.23	89.04
	CHG	157,148	0.51	2.44
	CHH	549,675	0.50	8.52
M-3nα	C	6,783,360	2.35	100
	CG	6,048,066	15.62	89.16
	CHG	162,808	0.51	2.4
	CHH	572,486	0.49	8.44
HPM-3n	C	6,333,697	2.19	100
	CG	5,556,871	14.02	87.74
	CHG	166,637	0.54	2.63
	CHH	610,189	0.54	9.63
F-2n	C	5,808,926	2.11	100
	CG	4,929,168	13.64	84.18
	CHG	172,073	0.50	3.07
	CHH	707,685	0.52	12.75
M-2n	C	6,435,338	2.22	100
	CG	5,778,594	15.26	89.79
	CHG	142,762	0.41	2.22
	CHH	513,982	0.40	7.99

*Each sample contains three replicates

The methylation profiles of TEs were also similarly detected to the gene regions and included both up-stream and down-stream regions. Similarly, the overall DNA methylation profiles were also consistent in both diploid and triploid oysters in TE regions (Figs. 1C and S1G–K). The CG sites showed higher methylation levels in TE gene body at the transcriptional initiation and termination points than in flanking regions, which was different from the genes (Fig. 1A, C). The methylation levels of CHG and CHH sites were similar at the transcriptional initiation and termination points, as well as across the gene body and flanking regions and showed an unchanged trend (Fig. S1L). To further describe the methylation profile within TEs, the methylation trend of long terminal repeats (LTRs), long interspersed elements (LINEs), short interspersed elements (SINEs), and DNA transposons were compared (see materials and methods). However, the methylation levels of TEs were different: SINEs showed the highest methylation levels, followed by DNA, and LINEs were the lowest (Fig. 1D). The methylation levels of CHG and CHH sites were low, and the same patterns existed in the gene regions and TE regions (Fig. S1F, L).

DNA Methylation Difference Between Diploids and Triploids

In this study, the methylation of the CG context has only been studied, if not specifically noted. To further comprehend the effect of ploidy on genome methylation, the mCG level at the whole-genome scale between diploid and triploid was compared. Interestingly, although four of them were triploids, the methylation levels of F-3nα, F-3nβ, M-3nα, and HPM-3n were quite different. F-3nα presented a higher methylation level than that in F-2n (Fig. S2A). In contrast, the methylation level of F-3nβ was lower than that of F-2n (Fig. 2A). Similar patterns of methylation were revealed in the group of M-2n-VS-M-3nα and M-2n-VS-HPM-3n (Figs. S2B and 2B). Then, the methylation differences were further analyzed between diploid and triploid oysters in genes and TEs. The methylation differences of diploids and triploids in gene regions were consistent with that of the whole genome, and F-3nβ and HPM-3n showed a low methylation level in each element of the gene (Fig. 2C and Table S3). Nevertheless, the methylation levels of SINEs in F-3nβ and HPM-3n were higher than that of F/M-2n and F/M-3nα, and DNA and LINEs methylation levels in HPM-3n were higher than that of M-2n, which was

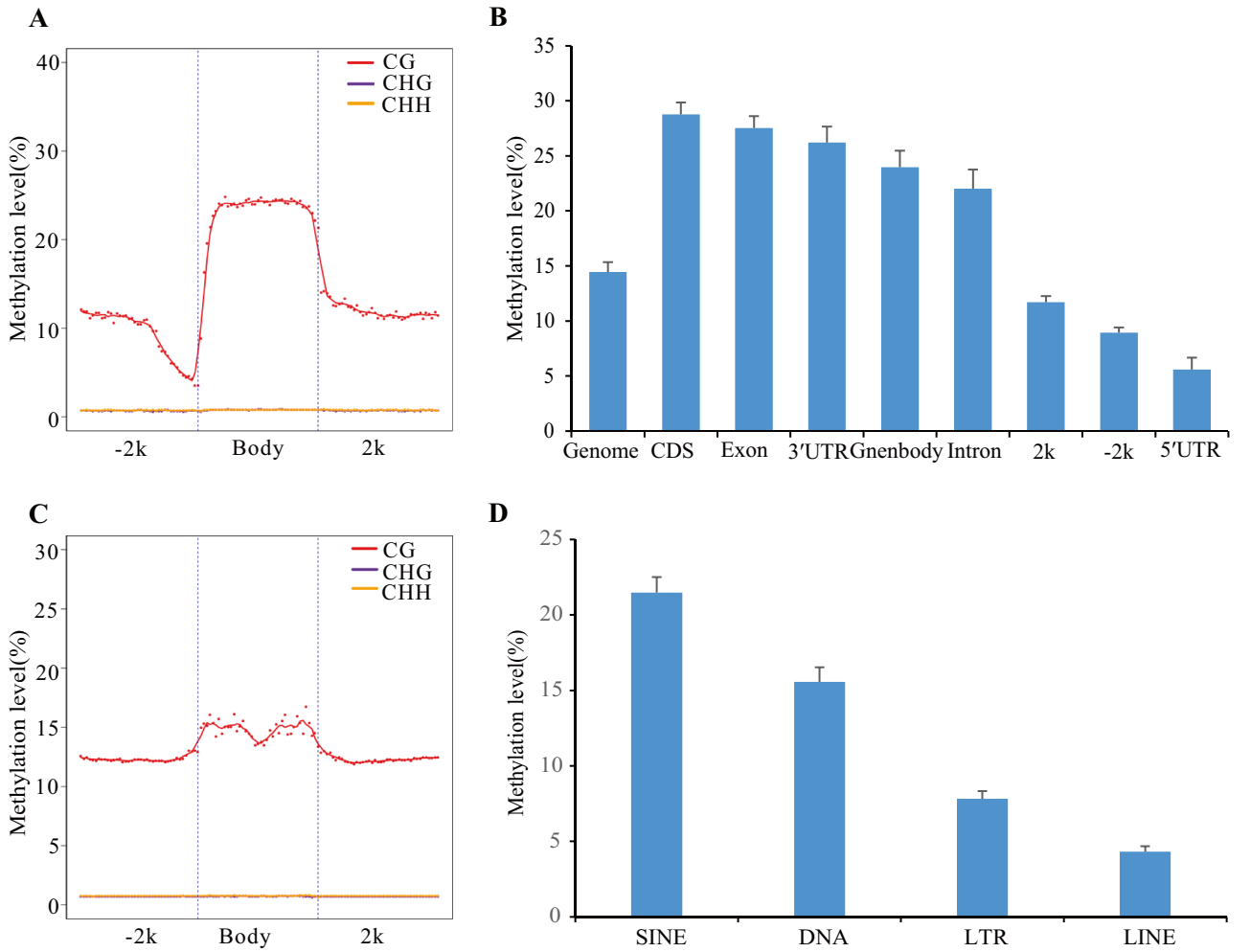

Fig. 1 DNA methylation patterns and DNA methylation levels of CG, CHG, and CHH contexts in gonads. **A**, **C** DNA methylation patterns of body regions (body), upstream-2 k (− 2 k) regions and downstream-2 k (2 k) regions in gene and transposable regions, respectively. **B**, **D** DNA methylation level of CG context in different parts of gene and transposable regions

contrary to the difference of overall methylation (Fig. 2D and Table S3). We subsequently investigated the regions that displayed significant methylation change among samples to identify differential methylation regions (DMRs) at CG sites. In total, 4409 (51% hyper and 49% hypo) DMRs were identified between F-2n and F-3nα, and 3806 (41% hyper and 59% hypo) DMRs were identified between F-2n and F-3nβ (Fig. 2E). In contrast, 17,741(12% hyper and 88% hypo) DMRs were identified between M-2n and HPM-3n, far more than that between M-2n and M-3nα, in which 3712 (61% hyper and 39% hypo) DMRs were found (Fig. 2E). More than 70% of DMRs occurred in the gene body in the four comparison groups, and 87% DMRs existed in gene body when compared HPM-3n with M-2n (Fig. S2C). The above results indicated that DNA methylation changed after polyploidization and the changes mainly occurred in methylation of F/M-3nα and demethylation of F-3nβ and HPM-3n.

Kyoto Encyclopedia of Genes and Genomes (KEGG) analysis was carried out to examine which biological and physiological pathways might be influenced by DMRs. We identified 1865, 1763, 1502, and 3337genes with DMRs in F-2n-VS-F-3nα, F-2n-VS-F-3nβ, M-2n-VS-M-3nα, and M-2n-VS-HPM-3n, respectively (see "Materials and Methods"). The KEGG analysis showed that the genes covered methylated regions were predicted to be involved in multiple physiological and biological pathways. A total of 199 (101 hyper and 98 hypo), 311 (127 hyper and 184 hypo), 231 (128 hyper and 103 hypo), and 1437 (222 hyper and 1215 hypo) genes in the four groups were significantly enriched into 21, 20, 18, and 58 pathways ($P < 0.05$), respectively (Table S4). The top five pathways involved in the four compare groups were nucleotide excision repair; steroid hormone biosynthesis; ribosome, alanine, aspartate, and glutamate metabolism; and fatty acid biosynthesis in F-2n-VS-F-3nα. Fatty acid biosynthesis, glycosaminoglycan

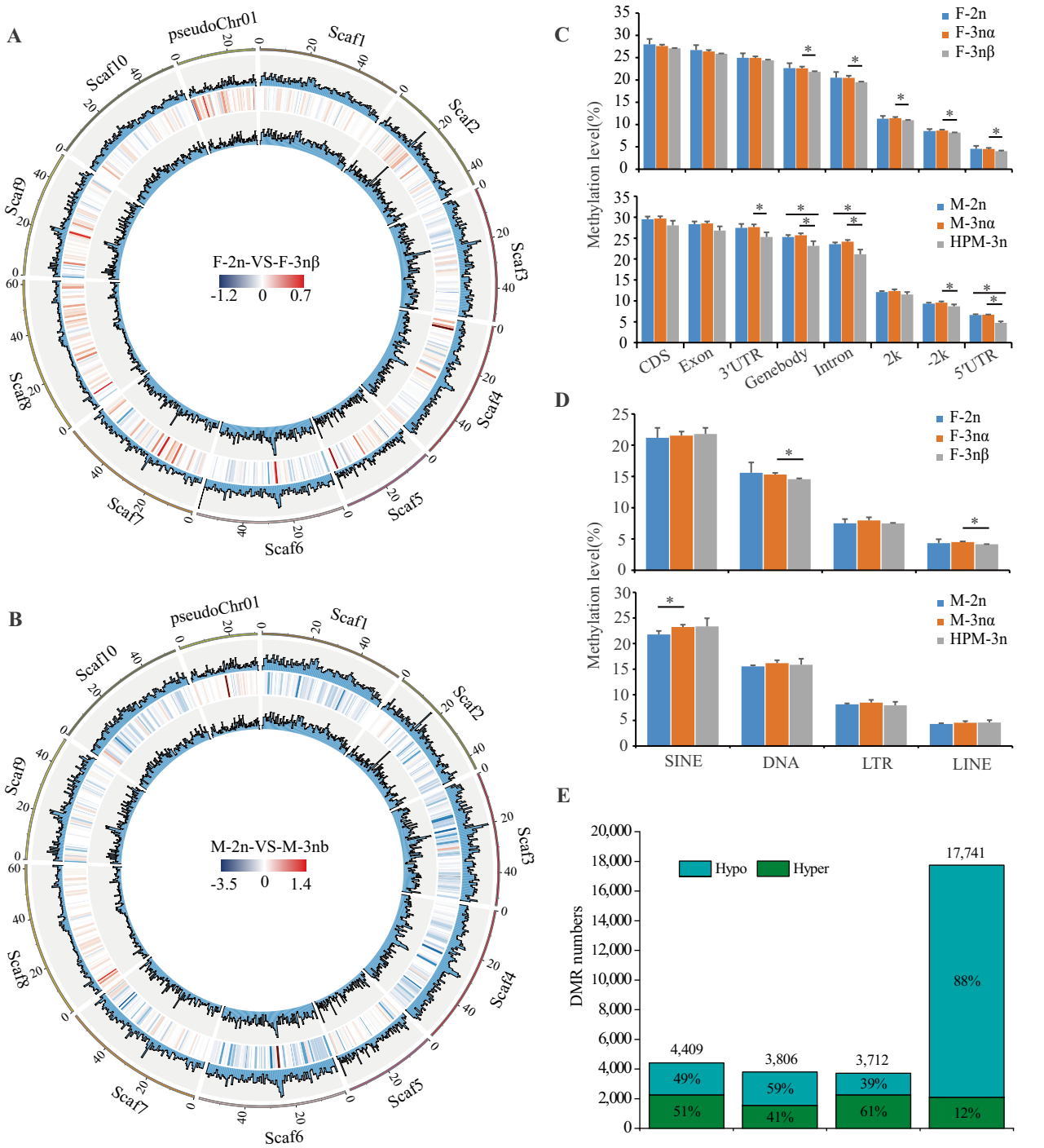

Fig. 2 Differences of DNA methylation at CG context. **A**, **B** Distribution of methylation levels in genome scaffolds. The outer ring of the circle plot represented the level of F-3nβ (**A**) and HPM-3n (**B**), the inner ring represented the methylation level of F-2n (**A**) and M-2n (**B**), and the intermediate heat map represented the differential methylation. Absolute value of the methylation rate difference more than 0.25 ($P < 0.05$) was the different methylated site. **C**, **D** Comparison of methylation levels of the six samples in genes or TEs. Asterisks indicate significant differences. **E** Numbers of differentially methylated regions (DMRs) of the four comparison groups and the proportions of hypermethylated (Hyper) and hypomethylated (Hypo) in each comparison group. **E** The proportion of upstream, gene body and downstream of gene region in each comparison group

biosynthesis-heparan sulfate/heparin, pyruvate metabolism, glycolysis/gluconeogenesis, and biosynthesis of unsaturated fatty acids in F-2n-VS-F-3nβ. Proteasome, ubiquitin-mediated proteolysis, MAPK signaling pathway-fly, nucleotide excision repair, and TNF signaling pathway in M-2n-VS-M-3nα. Chemokine signaling pathway, Fc gamma R-mediated phagocytosis, ErbB signaling pathway, MAPK signaling pathway-fly, and MAPK signaling pathway in M-2n-VS-HPM-3n (Table S4). All in all, the results suggested that the genes harbored DMRs might contribute to the alterations of gonadal development in triploid oysters after polyploidization, including the multiple metabolism pathways in F-3nβ and multiple signal pathways in HPM-3n.

Dynamic Expression of DNA Methylation and Demethylation Related Genes During the Gonadal Development

The dynamic changes of methylation were caused by DNA methyltransferase and demethylase activities, which have pivotal roles in reading and deleting of the DNA methylation during gonadal development. DNA methylation level could be changed by altered transcription levels of methylase genes. Thus, we detected the relative expression levels of methylation-related genes during the resting, proliferative, and mature stages of gonadal development. The DNA methylation–related genes encoding DNMT1 and DNMT3B were detected with the gonadal development by qPCR. Dynamic expression of DNMT1 gene was detected, and the expression of DNMT3B gene peaked during the proliferating phase of both diploid and triploid gonadal development, except for F-3nβ in mature phase (Fig. 3A, B). The gene expression level of UHRF1, a cofactor of DNMT1, increased gradually with the development stages, but was significantly lower than that of F/M-2n and F/M-3nα in F-3nβ and HPM-3n at mature stages ($P < 0.05$: Fig. 3A, B). TET3, TDG, and MBD4 were responsible for DNA demethylation. The expression level of *Tet3* was higher in the proliferative phase, and the expression level of TDG gene had a similar pattern, with the exception of the F-2n that showed

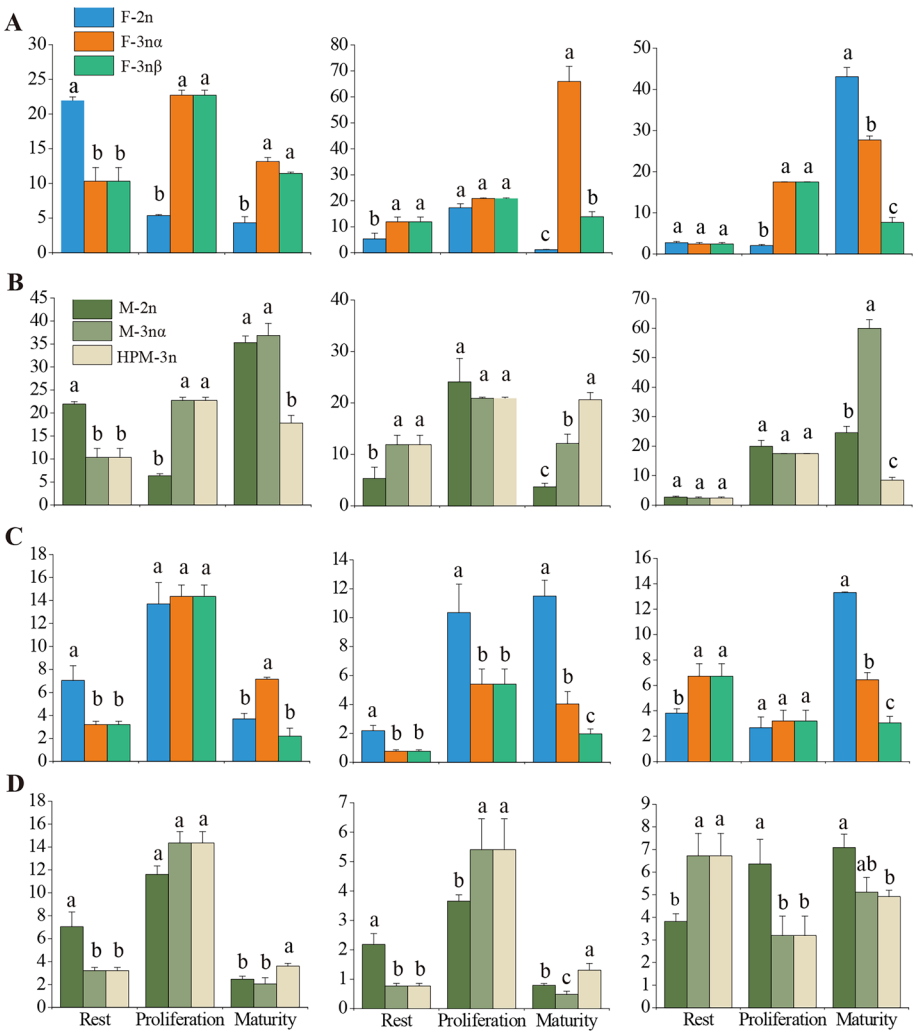

Fig. 3 The expression patterns of methylation-related genes in different developmental stages. **A**, **B** The gene expression of DNMT1, DNMT3B, and UHRF1 from left to right. **C**, **D** The gene expression of TET3, TDG, and MBD4 from left to right. Since gender could not be distinguished in diploid and triploid resting stage and triploid proliferating stage, the expression level of the same gene represented by the same value in the diploid and triploid resting period, and in the triploid proliferation period. Analysis of variance to test significance and significant differences were represented by different letters ($P < 0.05$) in the same stage. Each sample contains three replicates

high expression in mature stage (Fig. 3C, D). Therefore, the dynamic expression of methylation and demethylation genes with the gonadal developmental periods suggested the dynamic changes of DNA methylation during gonadal development. Meanwhile, the decrease of UHRF1 gene expression at mature stage might lead to the decrease of DNA methylation levels in F-3nβ and HPM-3n.

Gene Expression and DNA Methylation

To further examine the correlativity between DNA methylation and gene transcription level in gonads of oysters, total RNAs were isolated from the same samples and to perform to RNA-seq. The results of qPCR were consistent with the RNA-seq results, indicating the accuracy of the RNA-seq results (Fig. S3).

To investigate the relationship between DNA methylation and gene transcription level, we analyzed the correlation between gene expression level and DNA methylation level. Genes were separated into no expression, the lowest expression level, middle expression level, and highest expression level. No expression gene group presented lowest DNA methylation level in gene regions. Middle-expressed and high-expressed gene groups were related to high DNA methylation level in gene body, and the DNA methylation level of low-expressed was lower (Figs. 4A and S4). Whereas unapparent association was observed in the up and down stream-2 k regions of genes.

To further evaluate the relevance between gene expression and DNA methylation level, genes were divided into four groups on account of methylation level: non-methylation, low methylation, medium methylation, and high methylation levels. The methylation level in the entire gene region was positively correlated with gene transcription level (Figs. 4B and S4). Spearman's r was beyond 0.42 ($P < 10^{-15}$) between gene expression and DNA methylation in gene body of all samples (Figs. 4C and S4) and the weak positive correlation was uncovered between gene expression and DNA methylation in up- and down-stream-2 k. Taken in all together, gene transcription levels were generally positively associated with DNA methylation level of gene body region in a genome-wide scale.

DNA Methylation Regulated Metabolism Pathways in F-3nβ and Signal Pathways in HPM-3n

In total, 695, 5132, 709, and 2,288 differential expression genes (DEGs) were identified in F-2n-VS-F-3nα, F-2n-VS-F-3nβ, M-2n-VS-M-3nα, and M-2n-VS-HPM-3n, respectively. The number of DEGs suggested that the global transcriptome expression profiles were substantially changed in F-3nβ and HPM-3n. To further study whether DEGs were potentially affected by DMRs, we searched for the DEGs with DMRs and found that 42 (6.04%), 392 (7.64%), 31 (4.37%), and 338 (14.77%) DEGs were covered by DMRs in gene regions in the four groups analyzed above (Fig. S5).

Since DNA methylation existing in the gene body region was related to the facilitation of gene expression (Olson and Roberts 2014; Wang et al. 2014), we identified the DEGs covered by DMRs in the gene body region. We concerned the hypermethylated DMRs, which were related to upregulated DEGs and hypomethylated DMRs, which were related to downregulated DEGs. There were 11 and 45 hypermethylated DMRs in gene body region to upregulated DEGs, while 8 and 111 hypomethylated DMRs in gene body region were

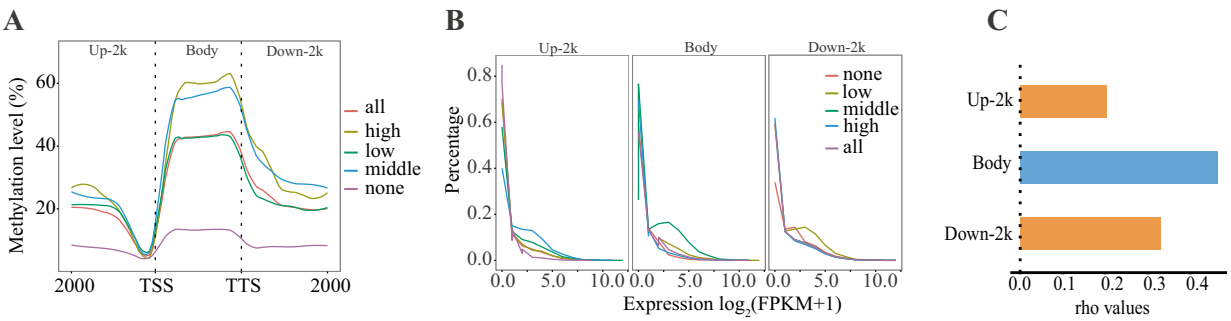

Fig. 4 Effect of DNA methylation of mCG on global gene expression in sample F-2n. **A** The *X*-axis represented the upstream and downstream positions of the gene, and the transcription initiation (TSS) and termination (TSS) sites respectively, and the *Y*-axis represented the average methylation level; different colors represented gene sets with different expression levels. None refer to FPKM ≤ 1, low refer to 1 < FPKM ≤ 10, middle refer to 10 < FPKM ≤ 100, and high refer to FPKM > 100, and all refer to all the genes. **B** The *X*-axis was the gene expression level (FPKM value + 1 was log), and the *Y*-axis was the gene frequency. Different colors represented different methylation levels. None refer to the non-methylated gene set, and the methylated level of methylated gene was divided into three groups, low refer to the low methylation gene set, middle refer to the medium methylation gene set, high refer to the high methylation gene set, and all refer to the all gene set. **C** The Spearman analysis between DNA methylation and gene expression. rho > 0 was positive correlation, rho < 0 was negative correlation. The remaining 5 samples is shown in Fig. S4

related to downregulated DEGs in the groups of F-2n-VS-F-3nα and F-2n-VS-F-3nβ, respectively (Fig. 5 and Table S5). In the groups of M-2n-VS-M-3nα and M-2n-VS-HPM-3n, 5 and 9 hypermethylated DMRs in gene body region were upregulated DEGs, while 8 and 160 hypomethylated DMRs in gene body region were related to downregulated DEGs, respectively (Fig. 5 and Table S5).

Due to the fertility and few DEGs covered with DMRs in F-2n-VS-F-3nα and M-2n-VS-M-3nα, only F-2n-VS-F-3nβ and M-2n-VS-HPM-3n were carried out for KEGG pathway enrichment analysis. The above DEGs associated with DMRs in gene body region were enriched in various KEGG pathways, including metabolic pathway, signaling pathway, and cell cycle (Table S6). One gene encoding origin recognition complex subunit 2-like (Fig. S6A–D) was hypomethylated and downregulated in F-3nβ, indicating that methylation might regulate gene expression and affected the initiation of DNA replication. Acetyl-coenzyme a synthetase 2-like gene (*Acss1*), which was hypermethylated and upregulated, and long-chain-fatty-acid–CoA ligase ACSBG2-like isoform X2 gene, which was hypomethylated and downregulated, were enriched in metabolism pathway, indicating that infertility in F-3nβ was associated with metabolic disorders induced by DNA methylation or demethylation. Interestingly, epigenetic regulation showed different regulatory mechanisms in the development of gametogenesis in females and males. The gene, M-phase inducer phosphatase-like isoform X1 (Fig. S6E–H), displayed demethylation and decreased expression level, suggesting that DNA methylation might control cell cycle progression by regulating gene expression. Additionally, the genes, sodium/calcium exchanger 2, cGMP-dependent 3′,5′-cyclic phosphodiesterase-like isoform X1, cyclic nucleotide-gated channel rod photoreceptor subunit alpha-like, and atrial natriuretic peptide receptor 1-like involved in cGMP-PKG signaling pathway, were all hypomethylated and downregulated, while the gene encoding tyrosine-protein kinase JAK2-like, which was involved in adipocytokine signaling pathway and Jak-STAT signaling pathway, was methylation and increased expression level, and these pathways or genes were related to the cell cycle. This indicated that infertility in HPM-3n was closely related to the regulation of cell signaling pathways, in which genes might be regulated by DNA methylation (Table S6).

Discussion

In this study, we used oyster as a model to characterize and compare the DNA methylation patterns of diploid and triploid oysters, and to provide insights into the epigenetic mechanism of infertile oysters. Our study provides a new mentality by using the models of fertility and infertility to investigate the regulatory mechanisms of gonadal development in invertebrates.

As observed from global DNA methylation, triploid oysters display mosaic methylation profiles with predominant methylation of gene body regions, in line with previous reports on diploid oysters and other invertebrates (Riviere 2014; Bonasio et al. 2012; Suzuki et al. 2007). In this study, the absence of the methylation in gene body regions of infertile triploid oysters may lead to various effects on the transcript, including access to alternative transcription start sites, increased sequence mutations, and alternative splicing (Roberts and Gavery 2012). Changes in the methylation of TE regions, especially the hypermethylation of SINEs (Fig. 2), whether results in alteration of transcripts or not is unclear. But the hypermethylation of SINEs is more associated to the characteristics of infertility, increasing

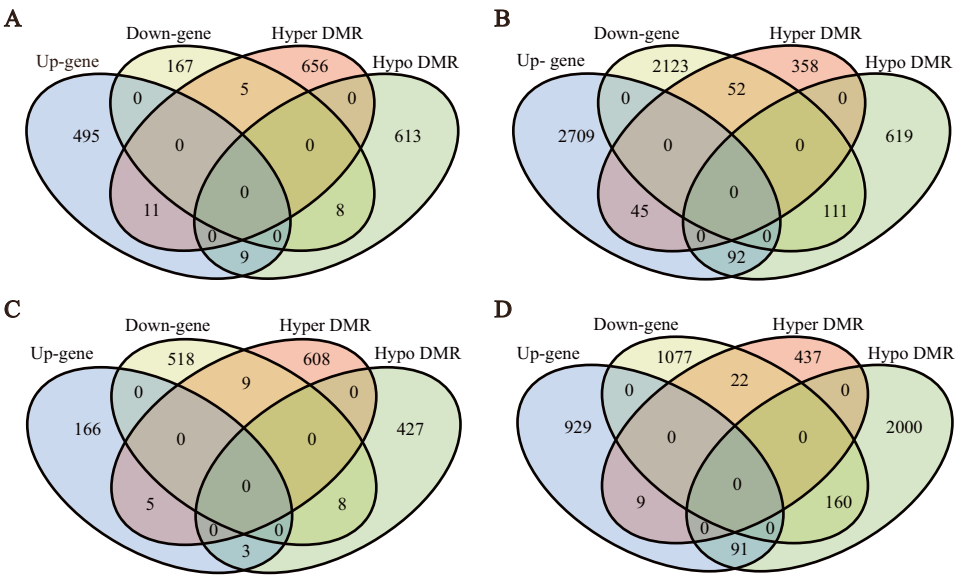

Fig. 5 Venn diagram showing the number of DMRs that occurred in gene body regions of DEGs. The number of upregulated genes (up-gene), downregulated genes (down-gene), hypermethylated DMRs (hyper DMR) and hypomethylated DMRs (hypo DMR) in F-2n-VS-F-3nα (**A**), F-2n-VS-F-3nβ (**B**), M-2n-VS-M-3nα (**C**), and M-2n-VS-HPM-3n (**D**)

the possibility that DNA methylation influences their expression. The overall methylation level decreases and local methylation level increases in triploid oysters observed in our study related to the results of interaction between methylase and demethylase (Fig. 3) (Lang et al. 2017; Zhang and Zhu 2012; De Riso et al. 2020).

In the well-studied polyploidy epigenetic modification, chromosome doubling can alter the DNA methylation that related to the change of phenotype (Liu et al. 2018; Yan et al. 2019; Xiao et al. 2013). In this study, the overall methylation levels in males were higher than that in females, and hermaphrodites were somewhere in between, indicating a correlation between gonadal development and DNA methylation in oysters, reminiscent of the recent findings in the coral reef fish (Todd et al. 2019). The proportion of incomplete methylation and distribution of methylation levels in HPM-3n were basically consistent with that in females (Figs. 6, S7 and S8. This suggests that the change of methylation in hermaphrodite predominantly males may affect gonadal development from male to female, consistent with the hypothesis that DNA methylation contributes to phenotypic plasticity (Roberts and Gavery 2012).

Throughout the evolution of species, mechanisms have emerged to store energy in the circumstances of food abundance and to prevent reproduction in the nutrient-deficient environment, especially in females (Fontana and Della Torre 2016). Gonadal development is a process from somatic cell growth to germ cell growth. However, the epigenetic instability of polyploids seems to be able to change the direction of development (Manor et al. 2015; Jouaux et al. 2013). In this study, the methylation levels of only 64 genes involved in metabolism pathways were changed in fertile triploid females, compared with 272 genes in sterile triploid females, which involved in the metabolism of carbohydrate, amino acid, and lipid (Table S4). The difference of metabolic genes caused by epigenetic instability may be related to distinct storage strategies observed between α and β triploids (Jouaux et al. 2013). Metabolic disorders can cause infertility, which is more thorough in mammals, especially in human studies (Fontana and Della Torre 2016). Furthermore, the genes covered with DMRs were significantly enriched in metabolic pathways related to oogenesis in infertility. For instance, in pyruvate metabolism (ko00620), five and nine genes were hypermethylated and hypomethylated, respectively, probably causing the disruption of the normal progress of pyruvate metabolism, which was essential for proper completion of oogenesis (Johnson et al. 2007).

Females account for a higher proportion in warm seasons with plenty of food that can influence the extent and rate of gametogenesis (Jouaux et al. 2013). In contrast, metabolic conditions do not seem to affect the gonadal development of males and HPM as much as females. In M-2n-VS-HPM-3n, genes covered with DMRs significantly enriched in 58 pathways, of which 22 were involved in signal pathways, while only five signaling pathways were significantly enriched in M-2n-vs-M-3nα (Table S4). mTOR signaling pathway, Wnt signaling pathway, and MAPK signaling pathway have specifically been associated with spermatogenesis among many species (Busada et al. 2015; Dong et al. 2015; Bogani et al. 2009; Amoyel et al. 2016). Methylation or demethylation occurring in genes enriched in signaling pathways may

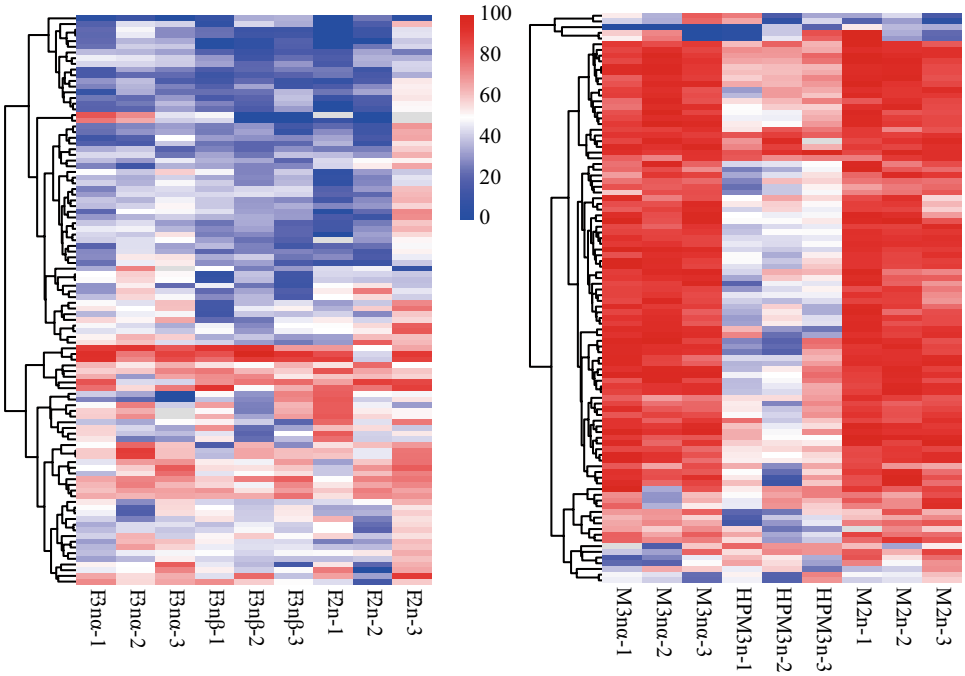

Fig. 6 CG DMRs heat map in all samples. Take the union of the DMR regions of all comparison groups and draw the heat map with the regional methylation rate of the top 100 DMRs

disturb the signaling transmission of gonadal development in HPM-3n.

Moreover, epigenetics also possesses a significant regulation effect on the process of mitotic cell proliferation and meiotic gametogenesis (Yamaguchi et al. 2012; Matsui and Hayashi 2007). Fifteen genes covered with DMRs were enriched in cell cycle pathway (ko04110) in F-2n-VS-F-3nβ, though not significantly (Table S4). These genes were involved in DNA replication (origin recognition complex subunit 2-like, DNA replication licensing factor mcm4-like, and zygotic DNA replication licensing factor mcm3-like), transcription (transcription factor Dp-1-like isoform X1), cell cycle checkpoint (S-phase kinase-associated protein 1 and cyclin-dependent kinase 6-lik), and chromosome separation (structural maintenance of chromosomes protein 5-like, anaphase-promoting complex subunit 1-like isoform X2, and anaphase-promoting complex subunit 7-like) in cell cycle. In *C. gigas*, oocytes undergo meiosis after discharging from gonads, while spermatocytes undergo meiosis in gonads. So, the triploid males must overcome the reproductive fitness problems caused by meiosis disorders (Wertheim et al. 2013; Comai et al. 2005). Previous study uncovered chromosomes in triploids could pass meiosis and produce gametes through mismatch repair mechanism in reptile (Spangenberg et al. 2017). In this research, the hypermethylated genes in nucleotide excision repair (ko3420) could be of functional significance for chromosomes passing through both meiosis divisions to produce gametes in M-3nα. Compared with gametogenesis of diploids, the slow development of gametes in triploids may be a strategy that circumvented the early challenge of polyploidization (Yan et al. 2019). Furthermore, 66% genes covered with DMRs enriched in cell cycle were hypomethylation in HPM-3n. This suggests that demethylation may be involved in gamete cell division and thus affect gonad development (Table S4).

Epigenetic modification plays a significant role in genome-wide reconstruction of transcriptional balance after polyploidization (Wertheim et al. 2013; Comai et al. 2005). A positive relationship between gene body methylation and gene transcription levels is uncovered in this study (Figs. 4 and S4), conforming to previous reports on oyster mantle, gills, or gametes (Wang et al. 2014, 2021; Olson and Roberts 2014; Riviere et al. 2017). DNA methylation occurring in promoter regions is believed to repress gene transcription in vertebrates (Siegfried and Simon 2010). However, lack of significant correlation between promoter methylation and mRNA transcription has been detected in invertebrates (Bonasio et al. 2012; Wang et al. 2014; Sarda et al. 2012) as well as in our study. This may be related to promoter hypomethylation in invertebrates (Jones 2012; Elango and Yi 2008), suggesting that the well-known gene regulation function of promoter methylation in plants and vertebrates may not work in invertebrates. Approximately 60–80% genes are managed by DNA methylation in plants and mammals (Yan et al. 2019; Zhang et al. 2019). In contrast, only 4–15% DEGs are regulated by DMRs in oyster gonads (Fig. S5), in line with the recent research on oyster gills (Wang et al. 2021). This difference may be related to the overall low methylation levels in invertebrates. So, both plasticity and stochasticity of gene expression in newly formed polyploids may be related to the DNA methylation variability.

Conclusions

In the present study, we obtained genome-wide methylation and transcriptome data of infertile and fertile oysters using whole genome bisulfite and RNA sequencing. The DNA methylation level of CG context decreases, with more hypomethylated than hypermethylated regions in infertile triploid oysters, and the opposite was true in fertile triploid oysters. The instability of epigenetic modifications involves in regulatory pathways related to fertility. In addition, the genes potentially regulated by DNA methylation were identified. Our research revealed the epigenetic mechanism of triploid infertility. This will aid better understanding of how epigenetic is involved in gonadal development and provides a new insight to explore the regulatory mechanisms of gonadal development in invertebrates.

Supplementary Information The online version contains supplementary material available at https://doi.org/10.1007/s10126-021-10083-y.

Funding This study was supported by grants from National Key R&D Program of China (2018YFD0900200) and National Natural Science Foundation of China (31672649).

Declarations

Conflict of Interest The authors declare no competing interests.

References

Amoyel M, Anderson J, Suisse A, Glasner J, Bach EA (2016) Socs36E controls niche competition by repressing MAPK signaling in the *Drosophila* testis. PLoS Genet 12:e1005815

Birchler JA, Yao H, Chudalayandi S (2007) Biological consequences of dosage dependent gene regulatory systems. Biochim Biophys Acta 1769:422–428

Bogani D, Siggers P, Brixey R, Warr N, Beddow S, Edwards J, Williams D, Wilhelm D, Koopman P, Flavell R A, Chi H, Ostrer H, Wells S, Cheeseman M, Greenfield A (2009) Loss of mitogen-activated protein kinase kinase kinase 4 (MAP3K4) reveals a requirement for MAPK signaling in mouse sex determination. PLoS Biol 7:e1000196

Bonasio R, Li Q, Lian J, Mutti NS, Jin L, Zhao H, Zhang P, Wen P, Xiang H, Ding Y, Jin Z, Shen SS, Wang Z, Wang W, Wang J, Berger SL, Liebig J, Zhang G, Reinberg D (2012) Genome-wide and caste-specific DNA methylomes of the ants *Camponotus floridanus* and *Harpegnathos saltator*. Curr Biol 22:1755–1764

Busada JT, Niedenberger BA, Velte EK, Keiper BD, Geyer CB (2015) Mammalian target of rapamycin complex 1 (mTORC1) is required for mouse spermatogonial differentiation in vivo. Dev Biol 407:90–102

Cavelier P, Cau J, Morin N, Delsert C (2017) Early gametogenesis in the Pacific oyster: new insights using stem cell and mitotic markers. J Exp Biol 220:3988–3996

Comai L (2005) The advantages and disadvantages of being polyploid. Nat Rev Genet 6:836–846

Conrad T, Akhtar A (2012) Dosage compensation in drosophila melanogaster: epigenetic fine-tuning of chromosome-wide transcription. Nat Rev Genet 13:123–134

Dong WL, Tan FQ, Yang WX (2015) Wnt signaling in testis development: unnecessary or essential?. Gene 565:155–165

De Riso G, Fiorillo DFG, Fierro A, Cuomo M, Chiariotti L, Miele G, Cocozza S (2020) Modeling DNA methylation profiles through a dynamic equilibrium between methylation and demethylation. Biomolecules 10:1271

Dheilly NM, Jouaux A, Boudry P, Favrel P, Lelong C (2014) Transcriptomic profiling of gametogenesis in triploid Pacific oysters *Crassostrea gigas*: towards an understanding of partial sterility associated with triploidy. PLoS One 9:e112094

Elango N, Yi SV (2008) DNA methylation and structural and functional bimodality of vertebrate promoters. Mol Biol Evol 25:1602–1608

Fontana R, Della Torre S (2016) The deep correlation between energy metabolism and reproduction: a view on the effects of nutrition for women fertility. Nutrients 8:87

Guo X, Allen SKJR (1994) Reproductive potential and genetics of triploid Pacific oysters, *Crassostrea gigas* (Thunberg). Biol Bull 187:309–318

Guo X, DeBrosse GA, Allen SK (1996) All-triploid Pacific oysters (*Crassostrea gigas* Thunberg) produced by mating tetraploids and diploids. Aquaculture 142:149–161

Hegarty MJ, Batstone T, Barker GL, Edwards KJ, Abbott RJ, Hiscock SJ (2011) Nonadditive changes to cytosine methylation as a consequence of hybridization and genome duplication in Senecio (Asteraceae). Mol Ecol 20:105–113

Johnson MT, Freeman EA, Gardner DK, Hunt PA (2007) Oxidative metabolism of pyruvate is required for meiotic maturation of murine oocytes in vivo. Biol Reprod 77:2–8

Jones PA (2012) Functions of DNA methylation: islands, start sites, gene bodies and beyond. Nat Rev Genet 13:484–492

Jouaux A, Blin JL, Adeline B, Heude-Berthelin C, Sourdaine P, Mathieu M, Kellner K (2013) Impact of energy storage strategies on gametogenesis and reproductive effort in diploid and triploid Pacific oysters *Crassostrea gigas* - involvement of insulin signaling. Aquaculture 388–391:173–181

Jouaux A, Heude-Berthelin C, Sourdaine P, Mathieu M, Kellner K (2010) Gametogenic stages in triploid oysters *Crassostrea gigas*: irregular locking of gonial proliferation and subsequent reproductive effort. J Exp Mar Biol Ecol 395:162–170

Lang Z, Wang Y, Tang K, Tang D, Datsenka T, Cheng J, Zhang Y, Handa AK, Zhu JK (2017) Critical roles of DNA demethylation in the activation of ripening-induced genes and inhibition of ripening-repressed genes in tomato fruit. Proc Natl Acad Sci USA 114:E4511–E4519

Lister R, Pelizzola M, Dowen RH, Hawkins RD, Hon G, Tonti-Filippini J, Nery JR, Lee L, Ye Z, Ngo QM, Edsall L, Antosiewicz-Bourget J, Stewart R, Ruotti V, Millar AH, Thomson JA, Ren B, Ecker JR (2009) Human DNA methylomes at base resolution show widespread epigenomic differences. Nature 462:315–322

Liu C, Wang M, Wang L, Guo Q, Liang G (2018) Extensive genetic and DNA methylation variation contribute to heterosis in triploid loquat hybrids. Genome 61:437–447

Mable BK (2004) 'Why polyploidy is rarer in animals than in plants': myths and mechanisms. Biol J Linn Soc 82:453–466

Madlung A (2013) Polyploidy and its effect on evolutionary success: old questions revisited with new tools. Heredity (edinb) 110:99–104

Manor ML, Weber GM, Cleveland BM, Yao J, Kenney PB (2015) Expression of genes associated with fatty acid metabolism during maturation in diploid and triploid female rainbow trout. Aquaculture 435:178–186

Mao X, Tao CJGO, Wei L (2005) Automated genome annotation and pathway identification using the KEGG Orthology (KO) as a controlled vocabulary. Bioinformatics 21:3787–3793

Matsui Y, Hayashi K (2007) Epigenetic regulation for the induction of meiosis. Cell Mol Life Sci 64:257–262

Okano M, Bell DW, Haber DA, Li E (1999) DNA methyltransferases Dnmt3a and Dnmt3b are essential for de novo methylation and mammalian development. Cell 99:247–257

Olson CE, Roberts SB (2014) Genome-wide profiling of DNA methylation and gene expression in *Crassostrea gigas* male gametes. Front Physiol 5:224

Otto SP, Whitton J (2000) Polyploid incidence and evolution. Annu Rev Genet 34:401–437

Pala I, Coelho MM, Schartl M (2008) Dosage compensation by gene-copy silencing in a triploid hybrid fish. Curr Biol 18:1344–1348

Piferrer F, Beaumont A, Falguière JC, Flajšhans M, Haffray P, Colombo L (2009) Polyploid fish and shellfish: production, biology and applications to aquaculture for performance improvement and genetic containment. Aquaculture 293:125–156

Ribas L, Vanezis K, Imues MA, Piferrer F (2017) Treatment with a DNA methyltransferase inhibitor feminizes zebrafish and induces long-term expression changes in the gonads. Epigenetics Chromatin 10:59

Riviere G (2014) Epigenetic features in the oyster *Crassostrea gigas* suggestive of functionally relevant promoter DNA methylation in invertebrates. Front Physiol 5:129

Riviere G, He Y, Tecchio S, Crowell E, Gras M, Sourdaine P, Guo X, Favrel P (2017) Dynamics of DNA methylomes underlie oyster development. PLoS Genet 13:e1006807

Roberts SB, Gavery MR (2012) Is there a relationship between DNA methylation and phenotypic plasticity in invertebrates?. Front Physiol 2:116

Sarda S, Zeng J, Hunt BG, Yi SV (2012) The evolution of invertebrate gene body methylation. Mol Biol Evol 29:1907–1916

Schultz MD, He Y, Whitaker JW, Hariharan M, Mukamel EA, Leung D, Rajagopal N, Nery JR, Urich MA, Chen H, Lin S, Lin Y, Jung I, Schmitt AD, Selvaraj S, Ren B, Sejnowski TJ, Wang W, Ecker JR (2015) Human body epigenome maps reveal noncanonical DNA methylation variation. Nature 523:212–216

Siegfried Z, Simon I (2010) DNA methylation and gene expression. Wiley Interdiscip Rev Syst Biol Med 2:362–371

Soltis DE, Soltis PS (1999) Polyploidy: recurrent formation and genome evolution. Trends Ecol Evol 14:348–352

Spangenberg V, Arakelyan M, Galoyan E, Matveevsky S, Petrosyan R, Bogdanov Y, Danielyan F, Kolomiets O (2017) Reticulate evolution of the rock lizards: meiotic chromosome dynamics and spermatogenesis in diploid and triploid males of the genus *Darevskia*. Genes (basel) 8:149

Suzuki MM, Kerr AR, De Sousa D, Bird A (2007) CpG methylation is targeted to transcription units in an invertebrate genome. Genome Res 17:625–631

Todd EV, Ortega-Recalde O, Liu H, Lamm MS, Rutherford KM, Cross H, Black MA, Kardailsky O, Marshall Graves JA, Hore TA, Godwin JR, Gemmell NJ (2019) Stress, novel sex genes, and epigenetic reprogramming orchestrate socially controlled sex change. Sci Adv 5:eaaw7006

Wang X, Li Q, Lian J, Li L, Jin L, Cai H, Xu F, Qi H, Zhang L, Wu F, Meng J, Que H, Fang X, Guo X, Zhang G (2014) Genome-wide and single-base resolution DNA methylomes of the Pacific oyster

Crassostrea gigas provide insight into the evolution of invertebrate CpG methylation. BMC Genomics 15:1119

Wang X, Li A, Wang W, Que H, Zhang G, Li L (2021) DNA methylation mediates differentiation in thermal responses of Pacific oyster (*Crassostrea gigas*) derived from different tidal levels. Heredity (edinb) 126:10–22

Wertheim B, Beukeboom LW, van de Zande L (2013) Polyploidy in animals: effects of gene expression on sex determination, evolution and ecology. Cytogenet Genome Res 140:256–269

Xiao J, Song C, Liu S, Tao M, Hu J, Wang J, Liu W, Zeng M, Liu Y (2013) DNA methylation analysis of allotetraploid hybrids of red crucian carp (*Carassius auratus* red var.) and common carp *(Cyprinus carpio* L.). PLoS One 8:e56409

Xi Y, Li W (2009) BSMAP: whole genome bisulfite sequence MAPping program. BMC Bioinformatics 10:232

Yamaguchi S, Hong K, Liu R, Shen L, Inoue A, Diep D, Zhang K, Zhang Y (2012) Tet1 controls meiosis by regulating meiotic gene expression. Nature 492:443–447

Yan H, Bombarely A, Xu B, Wu B, Frazier TP, Zhang X, Chen J, Chen P, Sun M, Feng G, Wang C, Cui C, Li Q, Zhao B, Huang L (2019) Autopolyploidization in switchgrass alters phenotype and flowering time via epigenetic and transcription regulation. J Exp Bot 70:5673–5686

Yue C, Li Q, Yu H (2018) Gonad transcriptome analysis of the Pacific oyster *Crassostrea gigas* identifies potential genes regulating the sex determination and differentiation process. Mar Biotechnol 20:206–219

Zhong S, Fei Z, Chen YR, Zheng Y, Huang M, Vrebalov J, McQuinn R, Gapper N, Liu B, Xiang J, Shao Y, Giovannoni JJ (2013) Single-base resolution methylomes of tomato fruit development reveal epigenome modifications associated with ripening. Nat Biotechnol 31:154–159

Zhang H, Zhu JK (2012) Active DNA demethylation in plants and animals. Cold Spring Harb Symp Quant Biol 77:161–173

Zhang X, Li Q, Kong L, Yu H (2018) DNA methylation frequency and epigenetic variability of the Pacific oyster *Crassostrea gigas* in relation to the gametogenesis. Fish Sci 84:789–797

Zhang X, Nie Y, Cai S, Ding S, Fu B, Wei H, Chen L, Liu X, Liu M, Yuan R, Qiu B, He Z, Cong P, Chen Y, Mo D (2019) Earlier demethylation of myogenic genes contributes to embryonic precocious terminal differentiation of myoblasts in miniature pigs. FASEB J 33:9638–9655